Population dynamics and wave propagation in a Lotka-Volterra system with spatial diffusion

Mao-Xiang Wang[1,2] and Pik-Yin Lai[1,*]

[1]*Department of Physics, Graduate Institute of Biophysics, and Center for Complex Systems, National Central University, Chungli, Taiwan 320, Republic of China*

[2]*School of Science, Nanjing University of Science and Technology, Nanjing 210094, China*

(Received 31 July 2012; revised manuscript received 10 October 2012; published 7 November 2012)

We consider the competitive population dynamics of two species described by the Lotka-Volterra model in the presence of spatial diffusion. The model is described by the diffusion coefficient (d_α) and proliferation rate (r_α) of the species α ($\alpha = 1,2$ is the species label). Propagating wave front solutions in one dimension are investigated analytically and by numerical solutions. It is found that the wave profiles and wave speeds are determined by the speed parameters, $v_\alpha \equiv 2\sqrt{d_\alpha r_\alpha}$, of the two species, and the phase diagrams for various inter- and intracompetitive scenarios are determined. The steady wave front speeds are obtained analytically via nonlinear dynamics analysis and verified by numerical solutions. The effect of the intermediate stationary state is investigated and propagating wave profiles beyond the simple Fisher wave fronts are revealed. The wave front speed of a species can display abrupt increase as its speed parameter is increased. In particular for the case in which both species are aggressive, our results show that the speed parameter is the deciding factor that determines the ultimate surviving species, in contrast to the case without diffusion in which the final surviving species is decided by its initial population advantage. Possible relations to the biological relevance of modeling cancer development and wound healing are also discussed.

DOI: 10.1103/PhysRevE.86.051908 PACS number(s): 87.23.Cc, 87.10.Ed, 87.17.Ee, 87.18.Hf

I. INTRODUCTION

The dynamics of population evolution has received a great deal of interest both theoretically and in experimental observations [1,2]. In particular the cooperative Lotka-Volterra (LV) model [3–5] is believed to be an appropriate model for a competitive community. While the dynamics and stability of the system in the case of well-mixed populations have been rather well described, the case in which the species can undergo spatial diffusion is less understood. The motion or migration of interacting species would produce important effects on the ecology of the system. The effects of species mobility modeled by spatial diffusion can result in possible wave fronts giving rise to interesting spatiotemporal dynamics. There have been several analytical studies focused on the stability of the LV system induced by diffusion. Vance and Allen showed that dispersal did not always promote the stability of the population [6,7]. Takeuchi and Hastings suggested that diffusion does not affect the system's stability [8,9].

It is known that for the LV model with diffusion, there exist traveling wave solutions propagating from one stationary point to another. At first glance, diffusion is a kind of random motion which should not be associated with directed motion. However, nonlinearity resulting from the interactions between the species can produce propagating waves, which travel much faster than the species' diffusional speeds. Such a propagating wave front represents a progressive replacement of one equilibrium (ahead of the front) by another (behind the front). So from the viewpoint of wave propagation, one can observe the stability of the system directly. On the other hand, previous research had been focused on the existence of traveling waves in the diffusive LV model. The simple Fisher's wave front can provide the connection of two states (one stable to the other unstable states) in part of the parameter space, but the intermediate equilibrium state is often overlooked or ignored. For the competitive diffusive LV model, there exists a combination of wave fronts as first mentioned by Tang and Fife in the uncoupled logistic growth model [10].

In this paper, we consider the LV model of two competitive species with spatial diffusion and investigate the steady wave front propagation not limited to the simple Fisher's waves. In particular, we examine the effect of intermediate equilibrium on the wave front profiles and wave speeds. Analytical results for the wave front and wave back speeds are obtained and verified by numerical solutions. It is found that not only dispersal but also proliferating rates affect the system's stability. In other words, it is the intrinsic speed parameters of these species that determine the population evolution and species domination or extinction.

II. COMPETITIVE LOTKA-VOLTERRA MODEL WITH SPATIAL DIFFUSION

We consider the two-species LV model with each species capable of undergoing spatial diffusion in one dimension. The populations of the two species are denoted by $n_1(x,t)$ and $n_2(x,t)$, obeying the reaction-diffusion type PDEs:

$$\begin{aligned} \frac{\partial n_1}{\partial t} &= d_1 \frac{\partial^2 n_1}{\partial x^2} + r_1 n_1 (1 - n_1 - a_{12} n_2), \\ \frac{\partial n_2}{\partial t} &= d_2 \frac{\partial^2 n_2}{\partial x^2} + r_2 n_2 (1 - n_2 - a_{21} n_1), \end{aligned} \tag{1}$$

where $d_\alpha > 0$ and $r_\alpha > 0$ ($\alpha = 1,2$) are the diffusion coefficients and growth rates, respectively. For the competitive LV model, both $a_{12}, a_{21} > 0$, and the environmental carrying capacity is taken to be 1. There are two kinds of competition among the members in the population: intraspecific competition and interspecific competition. The parameters a_{12}

*pylai@phy.ncu.edu.tw

determine the competitiveness of two different species. In this paper, we will consider systems in one dimension and investigate the associated wave propagations.

In the presence of diffusion, Eqs. (1) resemble the well-studied Fisher-Kolmogorov equation [11]. In the corresponding kinetic ODEs, steady states occur at the fixed points $(0,0),(1,0),(0,1),(n_1^*,n_2^*)$, where $n_1^* \equiv \frac{a_{12}-1}{a_{12}a_{21}-1}$ and $n_2^* \equiv \frac{a_{21}-1}{a_{12}a_{21}-1}$. The last steady state is only feasible when the densities of the populations are nonnegative. The study of wave fronts in Eq. (1) was initiated by Tang and Fife [10] who studied the wave front connecting from (0,0) to (n_1^*,n_2^*). Then other situations involved the wave fronts connecting two of the four equilibrium points: Gardner and Kan-on proved the existence of waves connecting the equilibrium states (1,0) and (0,1) [12–16]; Kanel and Zhou examined the two waves connecting the fixed points of (1,0) and (n_1^*,n_2^*) [17]. For the case involving three equilibrium points, Hosono transformed Eq. (1) into a three-dimensional ODE system and discussed the traveling wave fronts [18,19] connecting two stationary states. All these results merely demonstrated the existence of Fisher's wave fronts that connect two equilibrium fixed points. In this paper, using analytical and numerical methods, we investigate the stable propagating behavior beyond the simple Fisher's wave fronts.

A. The wave front speed constraint

We consider a local wave front that connects two equilibrium states X and Y as shown schematically in Fig. 1(a). For local wave front solutions, one writes $n_\alpha(x,t) = U_\alpha(x-ct)$, for $\alpha = 1,2$, for some wave front speed c to be determined. Then the reaction-diffusion type equations such as Eq. (1) will lead to a system of ODEs with dynamics described by (2) in a 4-dimensional phase space. Two fixed points in the corresponding 4-dimensional phase space of the dynamical system are denoted by $\mathbf{X}$ and $\mathbf{Y}$, and a propagating wave front of speed c is represented by a flow from $\mathbf{X}$ to $\mathbf{Y}$ as shown schematically in Fig. 1(b). Suppose the first two components in the phase space vector represent the population or concentration profiles; a physical requirement imposes that these population components be nonnegative. If the final fixed point $\mathbf{Y}$ consists of some zero population components, e.g., $\mathbf{Y} = (0,*,*,*)$, then the flow in phase space when approaching $\mathbf{Y}$ cannot spiral into $\mathbf{Y}$; otherwise some population components would be negative. The above physical requirement imposes a constraint on the eigenvalue of the Jacobian at $\mathbf{Y}$ and in turn results in a minimum constraint on the speed, $c \geqslant c_{\min}$. Furthermore, in many situations (as in all the scenarios in this paper), the stable wave front will select to propagate with the minimal speed $c_{\min}$. However, it should be noted that even though a wave front propagation is possible if there is a flow connecting from $\mathbf{X}$ to $\mathbf{Y}$, the stability of the wave front is not guaranteed but can be tested by numerical solution of the PDEs.

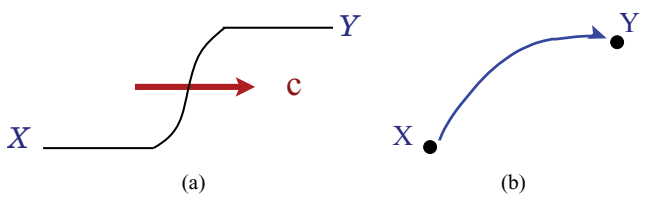

FIG. 1. (Color online) Schematics illustrating the wave front propagation for a wave front obtained by connecting the two equilibrium states. (a) Schematic wave front profile propagating with speed c. (b) 4-dimensional phase space flow from the fixed points $\mathbf{X}$ to $\mathbf{Y}$ resulting in a propagating wave front in (a).

Furthermore, in all the numerical solutions we obtained, the wave front always propagates with its minimal allowed speed and we never observe any steady wave front that propagates with some speed not constrained by an upper limit. Therefore, we shall adopt the conjecture that the wave front will propagate with its minimal constrained limit.

III. ANALYTICAL RESULTS FOR WAVE SPEEDS

In this section, the wave front speed constraints are derived analytically. Assuming local plane wave fronts with $n_1(x,t) = U_1(x-c_1t)$ and $n_2(x,t) = U_2(x-c_2t)$, Eqs. (1) are expressed as a four-dimensional first-order ODE dynamical system:

$$\begin{aligned} U_1' &= V_1, \\ U_2' &= V_2, \\ d_1V_1' &= -c_1V_1 - r_1U_1(1-U_1-a_{12}U_2), \\ d_2V_2' &= -c_2V_2 - r_2U_2(1-U_2-a_{21}U_1). \end{aligned} \tag{2}$$

This ODE system always has three fixed points $\mathbf{X_0} \equiv (0,0,0,0)$, $\mathbf{X_1} \equiv (1,0,0,0)$, $\mathbf{X_2} \equiv (0,1,0,0)$, and another fixed point $\mathbf{X_3} \equiv (n_1^*,n_2^*,0,0)$ emerges when both populations are nonnegative. Nonlinear dynamic is employed to analyze these fixed points one by one. The eigenvalues of the Jacobian at the fixed point $\mathbf{X_0} \equiv (0,0,0,0)$ obeys $[\lambda(\lambda+\frac{c_1}{d_1})+\frac{r_1}{d_1}][\lambda(\lambda+\frac{c_2}{d_2})+\frac{r_2}{d_2}] = 0$, which can be directly computed to give

$$-\frac{c_1}{2d_1} \pm \sqrt{\left(\frac{c_1}{2d_1}\right)^2 - \frac{r_1}{d_1}}, \quad -\frac{c_2}{2d_2} \pm \sqrt{\left(\frac{c_2}{2d_2}\right)^2 - \frac{r_2}{d_2}}. \tag{3}$$

It is clear that all the eigenvalues have negative real parts and the fixed point is stable. The physical requirement demands that the fixed point must be a stable node but not a stable spiral; otherwise regions with negative populations will result. So the wave speeds for the wave front ending with $\mathbf{X_0}$ must exceed the lower bound given by

$$c \geqslant \max[v_1,v_2], \tag{4}$$

where

$$v_\alpha \equiv 2\sqrt{d_\alpha r_\alpha}, \quad \alpha = 1,2, \tag{5}$$

is the "speed parameter" of the α species. It will be shown later that the phase diagrams for the wave profiles and all the wave front speeds are determined by the speed parameters of the two species.

For the fixed point $\mathbf{X_1}$, the eigenvalues can be similarly shown to obey $[\lambda(\lambda+\frac{c_1}{d_1})-\frac{r_1}{d_1}][\lambda(\lambda+\frac{c_2}{d_2})+\frac{r_2(1-a_{21})}{d_2}] = 0$,

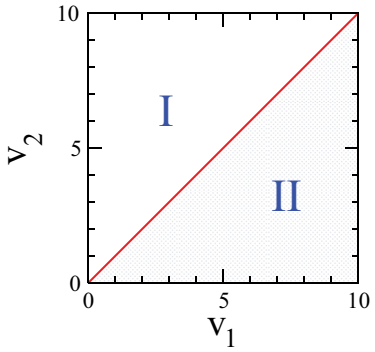

FIG. 2. (Color online) The phase diagram of steady wave propagation. Wave profiles are determined by the speed parameters of the two species, with two different wave properties separated by the boundary $v_2 = v_1$. The regions $v_1 < v_2$ and $v_2 < v_1$ are denoted by I and II, respectively.

which can be directly computed to give

$$2\lambda_{\pm}^{(1)} = -\frac{c_1}{d_1} \pm \sqrt{\left(\frac{c_1}{d_1}\right)^2 + \frac{4r_1}{d_1}},$$
$$2\lambda_{\pm}^{(2)} = -\frac{c_2}{d_2} \pm \sqrt{\left(\frac{c_2}{d_2}\right)^2 - \frac{4r_2(1-a_{21})}{d_2}}. \tag{6}$$

One can see that $\lambda_{\pm}^{(1)}$ is always real. But for $a_{21} < 1$, there is the possibility of $\mathrm{Im}\{\lambda_{\pm}^{(2)}\} \neq 0$ resulting in a spiral. So the physical requirement ensuring that $\lambda_{\pm}^{(2)}$ must be real leads to

$$c_2 \geqslant \sqrt{(1-a_{21})}v_2. \tag{7}$$

In this case, the fixed point $\mathbf{X_1}$ is a saddle, which has three stable directions and only one unstable direction. Similar analysis is applied to $\mathbf{X_2} \equiv (0,1,0,0)$ and one can get the wave speed constraints of n_1 to be

$$c_1 \geqslant \sqrt{(1-a_{12})}v_1. \tag{8}$$

$\mathbf{X_2}$ is also a saddle with three stable directions and one unstable direction. Finally, for the fourth fixed point $\mathbf{X_3}$, the eigenvalues cannot be expressed analytically, but they are given by the solution of the quartic polynomial equation

$$\lambda^2\left(\lambda + \frac{c_1}{d_1}\right)\left(\lambda + \frac{c_2}{d_2}\right) + \frac{r_1}{d_1}\lambda\left(\lambda + \frac{c_2}{d_2}\right)(1 - 2n_1^* - a_{12}n_2^*)$$
$$+ \frac{r_2}{d_2}\lambda\left(\lambda + \frac{c_1}{d_1}\right)(1 - 2n_2^* - a_{21}n_1^*)$$
$$+ \frac{r_1 r_2}{d_1 d_2}(1 - 2n_1^* - a_{12}n_2^*)(1 - 2n_2^* - a_{21}n_1^*)$$
$$- \frac{r_1 r_2 a_{12} a_{21} n_1^* n_2^*}{d_1 d_2} = 0, \tag{9}$$

and the numerical values of the eigenvalues and eigenvectors can be obtained precisely. This fixed point $\mathbf{X_3}$ does not set a limit to the wave speed, but the wave solution connecting these fixed points can become more complicated if $\mathbf{X_3}$ emerges. To get some insights about the wave front profiles, the PDEs in Eq. (1) are solved numerically, and the wave speeds are measured.

IV. NUMERICAL RESULTS

According to the phase plane analysis for the nondiffusive LV model, there are four situations, but these can be reduced to three cases without loss of generality: (1) interspecific competition in which one species dominates over the other: $0 \leqslant a_{12} < 1 < a_{21}$; (2) two populations coexisting: $0 \leqslant a_{12} \leqslant a_{21} < 1$; (3) interspecific competition in which both species are aggressive: $a_{12} \geqslant a_{21} > 1$. One can study the wave front profiles by numerically solving the PDEs in Eq. (1) for the above cases. Open boundary conditions are used. For convenience, time is in units of $1/r_1$ and space is in units of $\sqrt{d_1/r_1}$ in these numerical results. In all cases, the steady propagating wave profiles are determined by the speed parameters of the two species, and the phase diagram is shown in Fig. 2 with two different wave properties separated by the boundary $v_2 = v_1$.

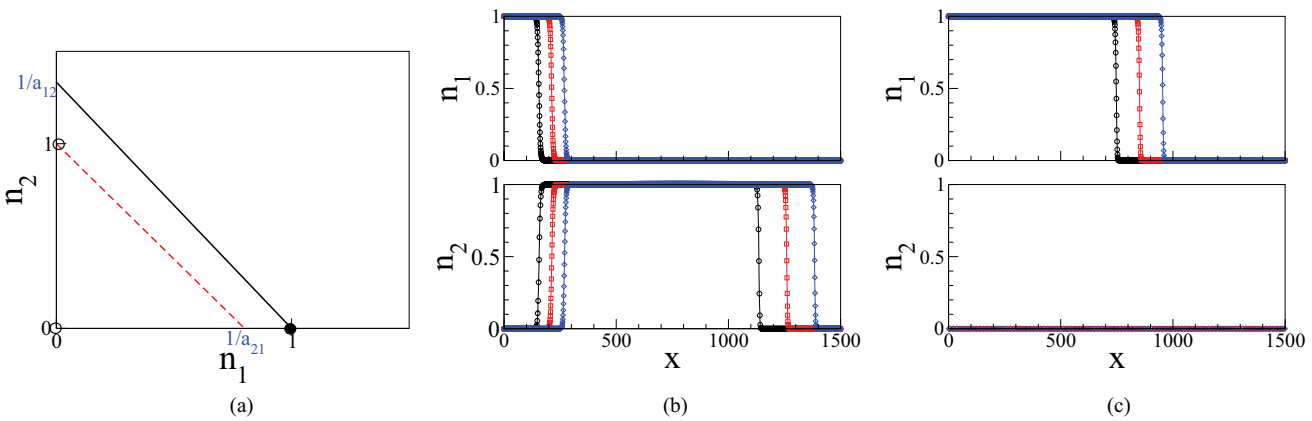

FIG. 3. (Color online) For the case $0 \leqslant a_{12} < 1 < a_{21}$, with $a_{12} = 0.75$. (a) The nullclines of the corresponding kinetic ODE system in Eq. (1); solid black and dashed red lines represent the nullclines of species 1 and 2. The stable and unstable fixed points are denoted by • and ○, respectively. (b) Steady wave front profiles in region I ($v_2 > v_1$) of the phase diagram Fig. 2. Wave profiles each separated by a time difference of 50 propagating in the $+x$ direction are shown. Time is in units of $1/r_1$ and space is in units of $\sqrt{d_1/r_1}$. (c) Similar steady wave front profiles in region II ($v_1 > v_2$) of the phase diagram.

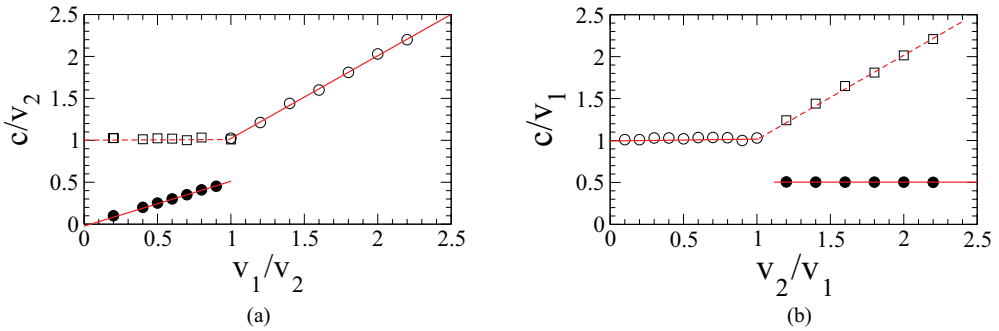

FIG. 4. (Color online) For the case $0 \leqslant a_{12} < 1 < a_{21}$, with $a_{12} = 0.75$. In this case, the wave front speeds are independent of the parameter a_{21}. Symbols in (a) and (b) are wave speeds measured from the numerical solutions. (○): Wave front speed of n_1. (□): Wave front speed of n_2. (●): Wave front speed of n_1 accompanied with the wave back of n_2 of the same speed. (■): Wave front speed of n_2 accompanied with the wave back of n_1 of the same speed. The solid and dashed lines in (a) and (b) are analytic results of the wave front speeds c_1 and c_2, respectively. (a) Wave front speeds vs the speed parameter v_1 for fixed value of v_2. In the $v_1 < v_2$ region, solid and dashed lines are $c_1 = v_1\sqrt{1-a_{12}}$ and $c_2 = \max(v_1, v_2) = v_2$, respectively. In the $v_1 > v_2$ region, solid line is $c_1 = \max(v_1, v_2) = v_1$. (b) Wave front speeds vs the speed parameter v_2 for fixed value of v_1. In the $v_2 < v_1$ region, solid line is $c_1 = \max(v_1, v_2) = v_1$. In the $v_2 > v_1$ region, solid and dashed lines are $c_1 = v_1\sqrt{1-a_{12}}$ and $c_2 = \max(v_1, v_2) = v_2$, respectively.

(1) $0 \leqslant a_{12} < 1 < a_{21}$. In this case the two species have opposite intra- and interspecific competitions. From the two-dimensional phase portrait for the LV model in Fig. 3(a), one can see that if the interspecific competition of one species dominates over the other, then the dominant species (the 1 species in this case) will become the final winner in the absence of spatial diffusion. But the above consequence can be quite different in the presence of diffusion. The steady propagating wave profiles are determined by the speed parameters of the two species separated by the boundary $v_2 = v_1$ as described by the phase diagram in Fig. 2. The wave profiles of the two species at three different times in the two regimes of the phase diagram are also shown in Figs. 3(b) and 3(c). In the $v_2 > v_1$ region (I), the dynamics can be described by the flow of fixed points: $\mathbf{X_1} \to \mathbf{X_2} \to \mathbf{X_0}$. The dynamics of the system is first attracted to the intermediate steady state (saddle fixed point) $\mathbf{X_2}$, leading to slow wave front of n_1 and the wave back of n_2 in the wave profiles. In the $v_2 < v_1$ region (II), the dynamics can be described by the flow of fixed points: $\mathbf{X_1} \to \mathbf{X_0}$. There is no doubt that the superior species (the 1 species) with high intrinsic speed will ultimately drive the other to extinction [see also Fig. 3(c) for the wave profiles]. But when the inferior species (the 2 species) has a larger speed parameter (i.e., $v_2 > v_1$, region I), then the two populations can coexist albeit in different regions, as shown in the wave profiles in Fig. 3(b). This interesting situation originates from their different intrinsic propagating speeds: The superior competitor owns a slow speed, but the inferior competitor can escape by propagating with a faster wave front while having a slower wave back of vanishing population as shown in Fig. 3(b). The wave back of the inferior species propagates with the same speed as the wave front of the superior species reflecting the fact that they are driven to extinction by the superior species. The faster speed of the inferior species is determined by the fixed point $\mathbf{X_0}$ and the superior population has the slow speed determined by the fixed point $\mathbf{X_2}$.

The steady wave front propagating speeds for both species are examined as functions of their speed parameters as shown

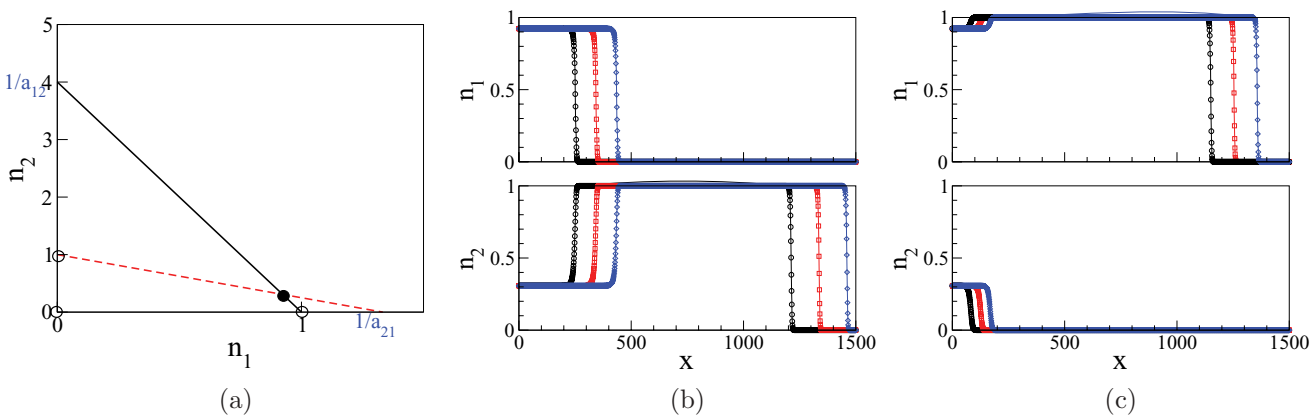

FIG. 5. (Color online) For the case $0 \leqslant a_{12} \leqslant a_{21} < 1$. (a) The nullclines of the corresponding kinetic ODE system in Eq. (1); solid black and dashed red lines represent the nullclines of species 1 and 2. (b) Steady wave front profiles in region I of the phase diagram Fig. 2. Wave profiles each separated by a time difference of 50 propagating in the $+x$ direction are shown. Time is in units of $1/r_1$ and space is in units of $\sqrt{d_1/r_1}$. (c) Similar steady wave front profiles in region II of the phase diagram.

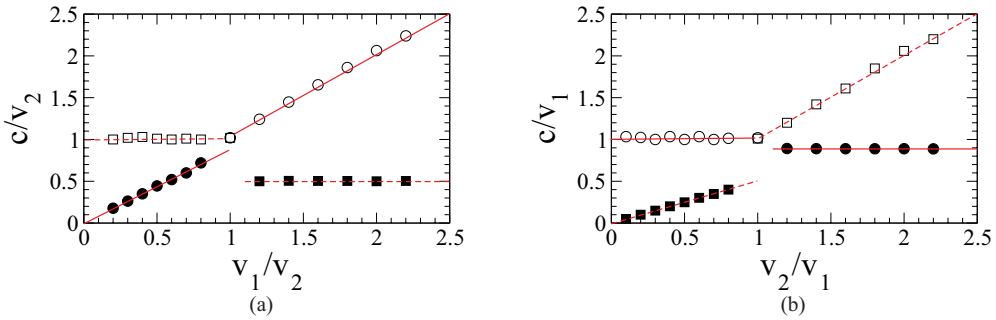

FIG. 6. (Color online) For the case $0 \leqslant a_{12} \leqslant a_{21} < 1$, with $a_{12} = 0.25$ and $a_{21} = 0.75$. Notations for the measured speeds and the analytic results are the same as in Fig. 4. (a) Wave front speeds vs the speed parameter v_1 for fixed value of v_2. In the $v_1 < v_2$ region, solid and dashed lines are $c_1 = v_1\sqrt{1-a_{12}}$ and $c_2 = \max(v_1,v_2) = v_2$, respectively. In the $v_1 > v_2$ region, solid and dashed lines are $c_1 = \max(v_1,v_2) = v_1$ and $c_2 = v_2\sqrt{1-a_{21}}$, respectively. (b) Wave front speeds vs the speed parameter v_2 for fixed value of v_1. In the $v_2 < v_1$ region, solid and dashed lines are $c_1 = \max(v_1,v_2) = v_1$ and $c_2 = v_2\sqrt{1-a_{21}}$, respectively. In the $v_2 > v_1$ region, solid and dashed lines are $c_1 = v_1\sqrt{1-a_{12}}$ and $c_2 = \max(v_1,v_2) = v_2$, respectively.

in Fig. 4. Figure 4(a) shows the wave front speeds as v_1 increases for a fixed value of v_2. The wave speeds are measured from the numerical solutions of Eq. (1) for waves that have attained their steady shapes. It is clear that the nature of the propagating waves shows a sharp change as v_1 increases across v_2. The wave front speeds as a function of v_2 for a fixed value of v_1 are also shown in Fig. 4(b). As shown in Fig. 4, the wave front speeds are well predicted by minimal speed values from the analytic results given by Eqs. (4), (7), and (8) in Sec. III.

Furthermore, it is worthwhile to note that for fixed v_2, as v_1 increases from small values, there is an abrupt jump in the wave front speed of the 1 species as its speed parameter exceeds v_2. The jump in wave front speed of the superior species can be obtained from the discontinuity of the speed as v_1 increases across the value of v_2, and is given by

$$\delta c = v_1(1 - \sqrt{1 - a_{12}}). \tag{10}$$

Such a scenario can be depicted by an analogy in the process of cancer development. One of the characteristics of cancer is uncontrolled growth and fast dispersal [20,21]. One can think of the cancer cells as being the superior species (1 species) in the sense that they have strong competition on normal cells (2 species). The case of low v_1 ($v_1 < v_2$) can be thought of as benign cancerous tumor cells in which they can proliferate but migrate with a slow speed and healthy cells can still grow. In the metastasis stage, the proliferation and/or migration of the cancer cells becomes active and its speed parameter increases. As v_1 becomes larger than v_2, there is a sharp increase in the propagation speed of the cancer cells by a factor of $1/\sqrt{1-a_{12}}$, and at the same time the cancer cells will occupy all the possible resources and suppress the growth of normal cells.

(2) $0 \leqslant a_{12} \leqslant a_{21} < 1$. In this case the interspecific competition is not so strong such that the two populations can coexist persistently, as depicted in the phase portrait in Fig. 5(a). Although the presence of diffusion does not change the stability of system, the wave fronts are different and can have different propagating speeds. Their propagating behavior is shown in Fig. 5, which is similar to the previous case of a superior competitor with a slow wave speed. The wave front also ends at the population fixed point (0,0) which determines the fast propagating speeds. The only difference is that the wave front profile starts from the new fixed point $\mathbf{X_3} \equiv (n_1^*, n_2^*, 0, 0)$ instead, and passes through the fixed point

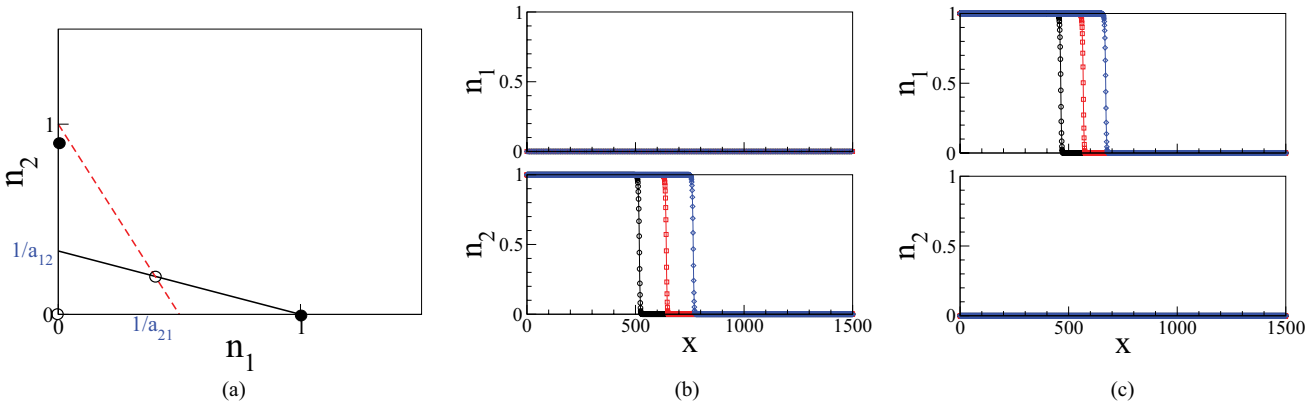

FIG. 7. (Color online) For the case $a_{12} \geqslant a_{21} > 1$, with $a_{12} = 3$ and $a_{21} = 2$. (a) The nullclines of the corresponding kinetic ODE system in Eq. (1); solid black and dashed red lines represent the nullclines of species 1 and 2. (b) Steady wave front profiles in region I of the phase diagram Fig. 2. Wave profiles each separated by a time difference of 50 propagating in the $+x$ direction are shown. Time is in units of $1/r_1$ and space is in units of $\sqrt{d_1/r_1}$. (c) Similar steady wave front profiles in region II of the phase diagram.

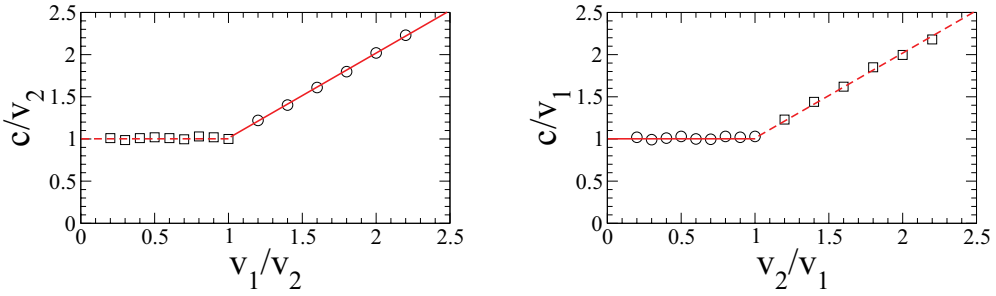

FIG. 8. (Color online) For the case $a_{12} \geqslant a_{21} > 1$. In this case, the wave front speeds are independent of the parameters a_{12} and a_{21}. Notations for the measured speeds and the analytic results are the same as in Fig. 4. (a) Wave front speeds vs the speed parameter v_1 for fixed value of v_2. Solid and dashed lines are $c_1 = \max(v_1, v_2) = v_1$ and $c_2 = \max(v_1, v_2) = v_2$, respectively. (b) Wave front speeds vs the speed parameter v_2 for fixed value of v_1. Solid and dashed lines are $c_1 = \max(v_1, v_2) = v_1$ and $c_2 = \max(v_1, v_2) = v_2$, respectively.

$\mathbf{X_1} \equiv (1,0,0,0)$ or $\mathbf{X_2} \equiv (0,1,0,0)$, which in turn sets the wave speed limit of the slow wave back. The slow wave back speed is the same as the propagating wave front speed of the other species. In the $v_2 > v_1$ region (I), the dynamics can be described by the flow of fixed points $\mathbf{X_3} \to \mathbf{X_2} \to \mathbf{X_0}$; in the $v_2 < v_1$ region (II), the dynamics can be described by the flow of fixed points $\mathbf{X_3} \to \mathbf{X_1} \to \mathbf{X_0}$. The steady wave front propagating speeds for both species are examined as functions of their speed parameters as shown in Fig. 6. Figure 6(a) shows the wave front speeds as v_1 increases for a fixed value of v_2. The wave speeds are measured from the numerical solutions of Eq. (1) for waves that have attained their steady shapes. Similarly to the previous case, the nature of the propagating waves shows a sharp change as v_1 increases across v_2. The wave front speeds are also well predicted by minimal speed values from the analytic results in Sec. III. Again there is a jump in the wave front speed of $\delta c_1 = v_1(1 - \sqrt{1 - a_{12}})$ for the 2 species as v_1 increases across v_2 [see Fig. 6(a)]. On the other hand, there is also a jump in the wave front speed of $\delta c_2 = v_2(1 - \sqrt{1 - a_{21}})$ for the 1 species as v_2 increases across v_1 [see Fig. 6(b)]. It is worthwhile to note that such a "shift of gears" in the abrupt change of wave front speed has also been observed in a recent reaction diffusion model involving cell differentiation [22].

The present scenario can be used to describe the process of wound healing [23] in which old cells (2 species) and newly proliferated cells (1 species) can coexist perpetually. Old cells have less competitive effect on the newly proliferated cells so as to assist the growth of new cells, and are modeled by the condition of $a_{12} < a_{21} < 1$. When there is a wound, the epidermal cell will begin its fast proliferation and undergoes migration. The other healthy cells properly reduce their growth speed which is determined by the competition of intra- and interspecific capacity as given by Eqs. (7) and (8).

(3) $a_{12} \geqslant a_{21} > 1$. In this case, the interspecific competition is aggressive. In the pure LV model without diffusion as depicted in the phase portrait in Fig. 7(a), ultimately one population wins while the other is driven to extinction and the winning species depends on which population has the starting advantage. However, in the presence of spatial diffusion, the situation can be quite different. The steady propagating wave profiles are also determined by the speed parameters of the two species, with the phase diagram in Fig. 2 with two different wave properties separated by the boundary $v_2 = v_1$. The wave profiles of the two species at three different times in the two regimes are also shown in Figs. 7(b) and 7(c). In the $v_2 > v_1$ region (I), the dynamics can be described by the flow of fixed points $\mathbf{X_2} \to \mathbf{X_0}$; in the $v_2 < v_1$ region (II), the dynamics can be described by the flow of fixed points $\mathbf{X_1} \to \mathbf{X_0}$. The wave front propagating behavior is relatively simple with one species propagating while the other species is swiped out to extinction. The steady wave front propagating speeds for both species are examined as functions of their speed parameters as shown in Fig. 8. In this case, the variations in the wave front speeds are simpler due to the fact that there is no intermediate steady state effect. Again the measured wave front speeds agree precisely with the theoretical values.

As noted above, in the presence of diffusion, our results indicate that the initial population has no priority and it is the propagating behavior that determines the ultimate winner. This can be verified through changing the initial conditions and following the evolution of population as shown in Fig. 9. It is

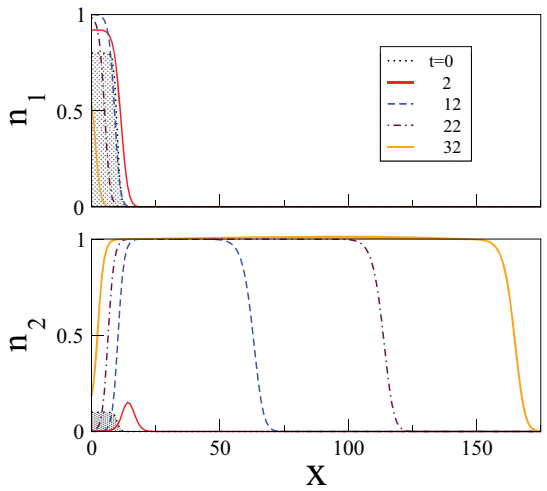

FIG. 9. (Color online) Time evolution towards steady plane wave front profiles obtained from numerical solution of Eq. (1) for the case of $a_{12} = 3 > a_{21} = 2 > 1$ and $v_1 = 4$, $v_2 = 10$. The initial densities are shown by the shaded regions with $n_1 = 0.8$ and $n_2 = 0.1$ in the same local region. Wave profiles at different later times are shown. Time is in units of $1/r_1$ and space is in units of $\sqrt{d_1/r_1}$.

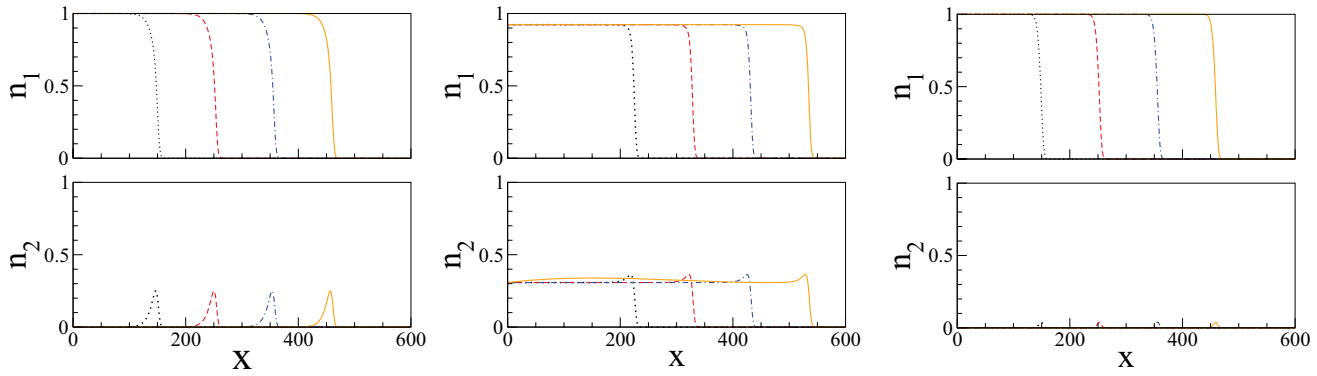

FIG. 10. (Color online) Steady plane wave front profiles obtained from numerical solution of Eq. (1) for the case of $v_1 = v_2$. Waves propagating in the $+x$ direction are shown. Time is in units of $1/r_1$ and space is in units of $\sqrt{d_1/r_1}$. (a) $0 \leqslant a_{12} < 1 < a_{21}$, with $a_{12} = 0.75$ and $a_{21} = 1.25$. The dynamics can be described by the flow of fixed points: $\mathbf{X_1} \to \mathbf{X_0}$. Four wave profiles each separated by a time difference of 50 are shown. (b) $0 \leqslant a_{12} \leqslant a_{21} < 1$ with $a_{12} = 0.25$ and $a_{21} = 0.75$. The dynamics can be described by the flow of fixed points: $\mathbf{X_3} \to \mathbf{X_0}$. (c) $a_{12} \geqslant a_{21} > 1$, with $a_{12} = 3$ and $a_{21} = 2$. The dynamics can be described by the flow of fixed points: $\mathbf{X_1} \to \mathbf{X_0}$.

clear from Fig. 9 that although species 1 has a local dominant population initially, the final winner is still species 2 if it has a larger speed parameter. The propagating behavior takes over the starting advantage in the deciding factor and determines the final survival species.

A. Two species having the same speed parameter

For the case in which the two species have exactly the same speed parameter, $v_1 = v_2$, the wave profile cannot be depicted by the profiles in the previous cases. In this case, the wave front speeds are all governed by the $\mathbf{X_0}$ fixed point, leading to $c_1 = c_2 = v_1 = v_2$. The steady propagating wave profiles for this special case are obtained from the numerical solution, and are shown in Fig. 10 for the three cases of different competitiveness. It is clear that although the two species propagate with very different wave profiles, they travel with the same wave speeds. For the case of $0 < a_{12} < 1 < a_{21}$, n_1 propagates with a step wave front whereas n_2 propagates with a small asymmetric pulse as shown in Fig. 10(a). Similar propagating profiles hold for the $a_{12} > a_{21} > 1$ case, but the pulse of n_2 is even more tiny as shown in Fig. 10(c). For the case of $0 < a_{12} < a_{21} < 1$, both n_1 and n_2 propagate with forward step wave fronts, with the shape of n_2 characterized by a small rising shoulder as shown in Fig. 10(b).

V. CONCLUSION AND OUTLOOK

For the LV competitive system, previous research was mostly concerned about the effect of dispersal on the system. But in practice proliferation and dispersal have equally important effects on the stability of system. Furthermore, the intermediate equilibrium plays an important role in the population dynamics, giving rise to wave propagation beyond the simple Fisher's wave fronts. Finally in the case of aggressive competition, the speed parameter, $v_\alpha \equiv 2\sqrt{d_\alpha r_\alpha}$, is the deciding factor for the surviving species instead of the initial population advantage, and dominates the dynamics of population evolution.

In this paper, only wave propagation in one dimension is considered. For population dynamics of interacting biological species on land, the two-dimensional case is relevant. For the two-dimensional case, although Eq. (1) does not admit an exact radial symmetric wave front solution, it can be shown easily using analysis similar to that in the standard Fisher-Kolmogorov equation [24] that the asymptotic solution admits a propagating wave front with speed bounds given by the one-dimensional results.

Only $N = 2$ species are considered in this paper; it is known that in the absence of spatial diffusion, the dynamics can be very rich for more interacting species. Without spatial diffusion, it has been shown that there is no limit cycle for the case of $N < 3$ and no chaotic dynamics for $N < 4$ [25], whereas for $N \geqslant 5$ all kinds of dynamics are possible [26]. It would be interesting to see the spatiotemporal patterns arising from the interplay of interactions for the cases of many species for $N \geqslant 3$.

ACKNOWLEDGMENT

This work has been supported by the NSC of the ROC under Grant No. NSC 101-2112-M-008-004-MY3, NCTS of Taiwan, and NSFC of China under Grant No. 11204132/A040102.

[1] H. I. Freedman, *Deterministic Mathematical Models in Population Ecology* (Marcel Dekker, New York, 1980).
[2] F. Brauer and C. Castillo-Chavez, *Mathematical Models in Population Biology and Epidemiology* (Springer-Verlag, New York, 2000).
[3] A. J. Lotka, J. Phys. Chem. **14**, 271 (1910).
[4] V. Volterra, in *Animal Ecology*, edited by R. N. Chapman (McGraw-Hill, New York, 1931).
[5] I. Bomze, Biol. Cybern. **48**, 201 (1983); **72**, 447 (1995).
[6] R. R. Vance, Am. Nat. **123**, 230 (1984).

[7] L. J. S. Allen, Math. Biosci. **65**, 112 (1983).
[8] Y. Takeuchi, Bull. Math. Biol. **48**, 585 (1986).
[9] A. Hastings, J. Math. Biol. **6**, 163 (1978).
[10] M. M. Tang and P. C. Fife, Arch. Ration. Mech. Anal. **73**, 69 (1980).
[11] R. A. Fisher, Ann. Eugenics **7**, 353 (1937); A. Kolmogorov, I. Petrovskii, and N. Piscounov, in *Selected Works of A. N. Kolmogorov*, Vol. 1, edited by V. M. Tikhomirov (Kluwer, Dordrecht, 1991), pp. 248–270.
[12] R. A. Gardner, J. Diff. Equ. **44**, 343 (1982).
[13] R. A. Gatenby, J. Theor. Biol. **176**, 447 (1995).
[14] R. A. Gatenby, Eur. J. Cancer **A32**, 722 (1996).
[15] Y. Kan-on, SIAM J. Math. Anal. **26**, 340 (1995).
[16] Y. Kan-on, Nonlin. Analysis TMA **28**, 145 (1997).
[17] J. I. Kanel and L. Zhou, Nonlinear Anal. TMA **27**, 579 (1996).
[18] Y. Hosono, Bull. Math. Bio. **60**, 435 (1998).
[19] Y. Hosono, in *Numerical and Applied Mathematics*, Part II, IMACS Annals on Computing and Applied Mathematics (Baltzer, Basel, 1989), pp. 687–692.
[20] L. Liu *et al.*, Proc. Natl. Acad. Sci. USA **108**, 6853 (2011).
[21] J. Y. Chang and P. Y. Lai, Phys. Rev. E **85**, 041926 (2012).
[22] M. X. Wang, Y. J. Li, P. Y. Lai, and C. K. Chan, preprint.
[23] M. Poujade *et al.*, Proc. Natl. Acad. Sci. USA **104**, 15988 (2007).
[24] J. D. Murray, *Mathematical Biology*, 3rd ed. (Springer, New York, 2002).
[25] M. Hirsch, SIAM J. Math. Anal. **16**, 423 (1985); Nonlinearity **1**, 51 (1988); SIAM J. Math. Anal. **21**, 1225 (1990).
[26] S. Smale, J. Math. Biol. **3**, 5 (1976).